Interacting localized structures with Galilean invariance

Christian Elphick
Physics Department, Universidad Técnica F. Santa María, Valparaíso 110-V, Chile

G. R. Ierley
Department of Mathematical Sciences, Michigan Technological University, Houghton, Michigan 49931

Oded Regev
Physics Department, Technion, Haifa 32000, Israel

E. A. Spiegel
Department of Astronomy, Columbia University, New York, New York 10027
(Received 31 January 1991)

We consider a nonlinear partial differential equation that arises in the study of Hopf bifurcation in extended systems, as in the Kapitza problem. The equation in one space variable and time has dispersion and dissipation, and it is invariant under translation and Galilean boost. This equation contains the Burgers, Korteweg–de Vries, and Kuramoto-Sivashinsky equations as special cases. Numerical studies reveal that the complicated solutions of this equation may be seen as a mixture of elementary, pulselike solutions that, in the course of time, lock in and form stable lattices for a wide range of system parameters. By describing such states as bound states of single pulses, we can calculate the lattice spacings accurately—a simple formula gives these spacings. We also use this multiparticle description to derive equations of motion of unbound, interacting pulses. These equations go to the proper asymptotic states and provide a qualitatively plausible description. However, some quantitative discrepancies with the numerical simulations suggest that further aspects of such problems deserve further exploration.

I. INTRODUCTION

The study of pattern dynamics has been advanced by the successful execution of experiments in one dimension (see the papers by Busse and Kramer [1]). A number of issues are raised by these experiments, including the formation and interaction of defects. In this paper, we shall be interested in the equations of motion of defects or other localized structures in systems with Galilean invariance. Such structures appear, for example, as special solutions of equations arising in the analysis of instability of extended systems [2]. An interesting example of such equations is

$$\partial_t u + u\partial_x u = \mathcal{P}u \ , \tag{1}$$

where $\mathcal{P}$ is a polynomial operator in ∂_x.

This equation descends from the complex, time-dependent Ginzburg-Landau equation when an equation for the phase ϕ of the order parameter can be filtered out [3]. Equation (1) for $u=\partial_x\phi$ then follows. Indeed, a number of special cases of such equations had already been studied back into the past century, before the current revival of interest occurred. The Burgers equation, with $\mathcal{L}=\partial_x^2$, appeared in Forsythe's book on differential equations and the Korteweg–de Vries (KdV) equation ($\mathcal{L}=\partial_x^3$) was derived in the context of shallow-water theory [4]. Another special case of more recent vintage is the Kuramoto-Sivashinsky (KS) equation [3], $\mathcal{L}=-\partial_x^2-\partial_x^4$, which has replaced the Burgers equation as a test problem for theories of turbulence.

In the present work, we focus on the nonlinear partial-differential equation (PDE)

$$\partial_t u + u\partial_x u + \nu\partial_x^2 u + \mu\partial_x^3 u + \lambda\partial_x^4 u = 0 \ , \tag{2}$$

derived by Benney [5] in the study of the instability of long waves on a thin layer of viscous fluid flowing down an inclined plane [6], the so-called Kapitza problem. More generally, (2) is the so-called phase equation for the study of Hopf bifurcation in a channel for an appropriate range of the system parameters.

The Burgers and KdV equations are completely integrable systems. They have scale invariances which enrich their dynamics, so we prefer the seemingly more complicated example, (2), though the KS equation would also suit our purposes. Numerical studies of (2) exist [7,8], showing that for certain initial conditions the system evolves to a steady state consisting of a train of solitary pulses at fixed spacings with saturated amplitudes. We aim here to extend the literature of reliable numerical studies of (2) and to increase our theoretical understanding of such results. Our numerical results confirm that the solutions of (2) do tend to form stable lattices of pulses that are steady in some particular frame.

Our theoretical treatment of (2) is based on the idea that it has features in common with many other problems involving localized or solitary structures formed in extended systems under the combined effects of instability and dissipation [9]. When the lifetime of such structures is long enough, the effective-particle approach used for

 ©1991 The American Physical Society

integrable systems [10] and in quantum field theory [11] can be extended to such systems. This approach is advantageous when the original system has one or more symmetry groups. For then, each solitary structure can be assigned a set of values of the group parameters and these become collective coordinates characterizing the state of the system [12,13]. In this way, many of the nonlinear PDE's encountered in macroscopic physics can be reduced to systems of ordinary differential equations (ODE's).

Methods of this general kind have been developed for dissipative, unstable systems possessing translational invariance in diverse problems [14,15]. However, such methods have not yet been systematically applied to systems with Galilean invariance. Of course, this extension poses no difficulty for integrable systems [16,17] where the inverse-scattering transform may be used, but it is not evident how to extend that procedure [18] into a method for the N-structure problems of pattern formation. Accordingly, we aim here to describe the dynamics of interacting localized structures with Galilean invariance using the effective-particle approach, along the lines discussed by Kawahara and collaborators [8,19], among others. Our approach is more systematic and our equations of motion differ from theirs. As we shall see, the fact that the pulses do not have fore-aft symmetry makes for complications in the dynamics that do not seem to have been previously appreciated. In contrast with some earlier descriptive analyses of numerical n-particle solutions, we concentrate here upon a narrower study of the complete family of two-particle solutions, testing for precise agreement with our predictions. In the characterization of the bound-state problem, we are successful in this, while in the dynamical description, we are considerably less so. Of course, common to *any* particle description of a system such as this is the occurrence of a constellation of fixed points of saddle and nodelike character which, in and of itself, cannot be regarded as a satisfactory theory without close agreement with calculated eigenvalues from the partial-differential equation.

We should mention at the outset an issue that remains open in all the discussions of such problems and that we do not discuss here—namely the difficulty caused by the fact that we must leave open the number of individual pulses that occur. We have as yet no means of describing the creation and destruction of pulses in these dissipative problems. Our aim here is the more limited one of describing the ultimate behavior of a fixed number of pulses.

II. USEFUL PRELIMINARIES

A. Localized structures

We substitute $u(x,t)=H(\xi)$, where $\xi=x-ct$, into (2), we get an ODE for H that we may integrate once to obtain

$$\lambda H'''+\mu H''+\nu H'+\tfrac{1}{2}H^2-cH=0\ . \tag{3}$$

The choice of zero integration constant is equivalent to choosing boundary conditions for which H vanishes when $\xi\rightarrow\pm\infty$, which amounts to putting the system into a selected inertial frame. (In the numerical solutions, where we work with periodic boundary conditions, it is convenient to fix the phase of the solution instead of the integration constant. In addition, the velocity, u, we use here is not necessarily the value seen in the laboratory. In the Kapitza problem, for example, velocities in (2) are referred to a particular moving frame with velocity $V=F\sqrt{gh}\cos\theta$, where F is the Froude number, θ the inclination angle, h the unperturbed height, and g the acceleration due to gravity. Thus in comparison with laboratory (fixed-frame) coordinates, the variable x is really $x-Vt$.) We shall refer to (3) as the *associated* ODE. It has both periodic and chaotic solutions [20] and this richness foreshadows the complexity we find in (2).

The solutions connecting the fixed points in the phase space of (3) to each other (heteroclinic) or to themselves (homoclinic orbits) describe localized structures in (2). Figures 1 and 2 show examples of the two main types of localized structure, the front [4] and the pulse [20]. In each, there is a core of characteristic width, σ, where the properties change rapidly. When the ODE is autonomous, the pulse or front typically approaches its asymptotic values exponentially as $\xi\rightarrow\pm\infty$. Because of the invariance properties of (2), if $H(\xi)$ is a solution, then so are $H(\xi-Y)$ and $H(\xi-X)+V$, where Y and V are constants and $\dot{X}=V$.

The ODE (3) has two fixed points; one is at the origin and the other has the coordinates $(H,H',H'')=(2c,0,0)$. The pulse shown in Fig. 2 is associated with an orbit leaving the origin exponentially in ξ, looping once around the other fixed point, and spiraling back to the origin. There also exist homoclinic orbits (localized structures) with multiple pulses, corresponding to two or more loops around the second fixed point.

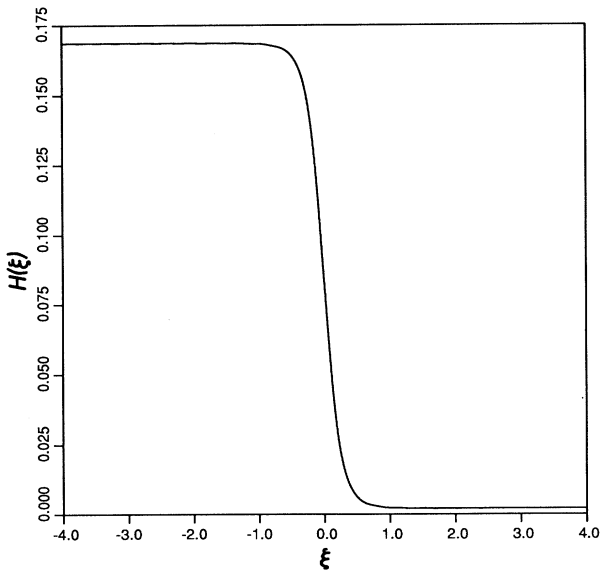

FIG. 1. Localized structure arising in (3) as a heteroclinic orbit (front) for $\lambda=0$, $\mu=0$, and $\nu=-0.02$.

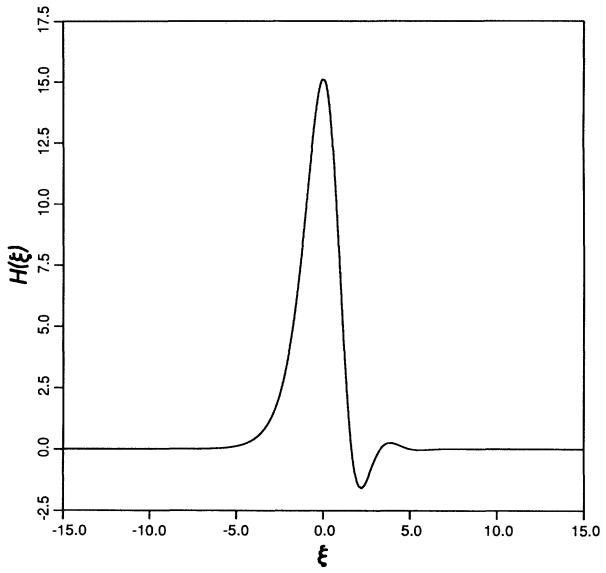

FIG. 2. Localized structure arising in (3) as a homoclinic orbit (pulse) for $\lambda=1$, $\mu=1$, and $\nu=2$.

B. A constraint

The numerical study of (2) serves as the experiment for which the theory of this paper is constructed. If we use periodic boundary conditions in the numerics, we get validity of the numerical results for the longest possible times. So we have mainly used periodic boundary conditions in our simulations. (We have also done a few computations using an algebraic map of the infinite interval into a finite domain. Rabinovich [21] reports successful use of absorbing boundary conditions with pulses propagating into the boundary and reflecting less than 1% of the energy incident. Apart from the periodic case, elementary homogeneous boundary conditions on a finite domain generally result in wave generation at the boundary for this nonlinear fourth-order problem.) The single- and multiple-pulse solutions which result with these boundary conditions cannot be precisely identified with the homoclinic and heteroclinic orbits of the associated ODE, except in the limit of infinite period. Thus, differences between scattering experiments on (2) and predicted solutions from ODE's derived in Secs. IV and V for the group parameters are expected. They are attributable both to the finite computational domain of the former and the finite order of truncation of the latter. We estimate the numerical errors to be much smaller than either of these effects.

In the numerics, we shall work on a domain of size L. Whether we have either (a) periodic boundary conditions or (b) infinite L with u and its spatial derivatives vanishing at infinity, we deduce from (2) that

$$\mathcal{I}\equiv\int_0^L u\,dx \tag{4}$$

is a conserved quantity. By means of a Galilean boost we can always arrange for $\mathcal{I}$ to be zero, but the figures showing our numerical results do not all conform to this choice.

We shall seek solutions which remain bounded and so will expect that the derivatives of u vanish at spatial infinity. Then, because of (4), we find from (2) that

$$\lim_{x\to+\infty} u^2=\lim_{x\to-\infty} u^2=0\ . \tag{5}$$

C. Pulse stability

In the theoretical developments to follow, we shall not make use of the exact multipulse solutions of the associated ODE. Instead, we shall construct all such solutions from the single pulse shown in Fig. 2. As this is the building block of our entire "edifice," it is desirable that it should have a reasonably long lifetime. Just as it would be of little value to try to make a nucleus from protons that lived only a very short time, so too is it futile to make patterns from pulses that are too short lived. This leads us to consider the stability of the localized structures. We test the stability of a solution of (2) of the form $u_L(x,t)=U(x-ct)$ for varying L with periodic boundary conditions. This fits in with our studies of time-dependent solutions to (2), which are also made with periodic boundary conditions.

We first show the loss of stability of the vacuum state (no pulses) using the energy method [22]. Multiplication of (2) by u and integration over the domain $[-L/2, L/2]$ gives

$$\frac{1}{2}\frac{d}{dt}\langle u^2\rangle=\frac{4\nu}{L^2}\langle u_z^2\rangle-\frac{16\lambda}{L^4}\langle u_{zz}^2\rangle\ , \tag{6}$$

where

$$\langle f\rangle=\tfrac{1}{2}\int_{-1}^{1} f(z)dz,\quad z=2x/L \tag{7}$$

and the subscript z denotes partial differentiation.

Let $u=U+v$ where U is a constant. We can readily derive an equation for the perturbation energy v^2 from (2). In the time-independent version of that equation we can show that L must conform to the condition

$$L^2=\min_v \frac{4\lambda}{\nu}\frac{\langle v_{zz}^2\rangle}{\langle v_z^2\rangle}\ . \tag{8}$$

By solving this problem, we can bound from below the L needed for a nontrivial v, even though the v which results from this is not constrained to satisfy the full equation, but only its second moment. This is a standard variational problem leading to an elementary Euler-Lagrange equation.

The ratio in (8) is minimized by taking $v=\cos(n\pi z+\vartheta)$ (with arbitrary phase ϑ). This gives a sequence of values $L_n=2n\pi\sqrt{\lambda/\nu}$. (For $L<L_1$, only the constant solution can exist.) Above L_1, the constant solution may become unstable to a finite disturbance which evolves to a single-pulse form of solution. For $L>L_n$, solutions ranging from one to N pulses are all possible, the multipulse solutions being simply the periodic extension of the

single-pulse case. [Other multipulse solutions of (3) in a periodic domain exist which are not directly accessible by the energy method. The family of such solutions representing a two-pulse state is presented later in the paper.]

As a complement to this calculation, we may perform a linear-stability analysis on (2) to discover the domain size above which an infinitesimal perturbation will grow. The critical L is the same since the bifurcation is supercritical. This is what happens in other familiar bifurcation problems such as the the Boussinesq convection problem. We can thus be certain that L_1 is the exact stability boundary for the vacuum solution, which is a constant. Elementary manipulation of the linear problem yields the added result that the velocity of the disturbances unstable on the vacuum is given by $c=-\nu\mu/\lambda$.

A similar analysis permits us to find the stability of the finite-amplitude single- and multiple-pulse states themselves with the help of numerical methods. For the linear-stability problem, with $v \propto \exp(st)$, we have the following eigenvalue problem:

$$sv=-\{L^{-1}[(U-c)\partial_z+U_z] +\nu L^{-2}\partial_z^2+\mu L^{-3}\partial_z^3+\lambda L^{-4}\partial_z^4\}v \ , \tag{9}$$

where $z=x-ct$. For U we may take single- or multiple-pulse solutions. For given ν, μ, and λ, we solve this problem, looking for the range of L over which the real part of s is negative. Outside of this range, the given basic state is always unstable. The energy method can be applied to the single- and multiple-pulse solutions, but is uninformative. As the domain size increases we find, as have Toh and Kawahara [7] that, in general, several stable equilibrium solutions can exist. In this circumstance no state can be stable with respect to disturbances of arbitrary amplitude.

As we shall also see the $2N$-dimensional phase space based upon positions and velocities of N pulses is constrained in its linear-stability properties to a discrete spectrum of excitations. Hence a full description of the dynamics contained in the partial-differential equation may not be possible in such terms. This is a question of current interest in problems of macroscopic physics and we are especially interested in seeing how far we can go in representing the numerical experiments by a description in a discrete set of collective coordinates.

III. NUMERICAL STUDIES

Steady traveling-wave solutions of (2) in a periodic domain are found by straightforward application of Newton's method to the associated ODE, (3). The solution is represented in a Chebyshev expansion. (For periodic boundary conditions a Fourier representation would work as well. Chebyshev polynomials were chosen to facilitate accurate treatment of several possible boundary conditions at an early stage in the work. In preliminary work, we also used a finite-difference shooting method, which performed satisfactorily. For time stepping, it is convenient to use a representation requiring a minimal number of variables.) An advantage of Newton's method is that, in the process of solution, it naturally produces the derivative matrix which, on incorporation of boundary conditions, determines the eigenspectrum of the linear-stability problem.

To present the results, we use the separation of the successive pulses in a wave train. If there are N pulses in the domain of size L, there are $N-1$ independent pair separations. Steady (in some frame), bound arrays of pulses can therefore be described in an N-dimensional space, if we include L in this description. Thus, for the case of a pair of pulses, the bound states are characterized by a pair of values: q, the pulse separation, and L, the domain size. The operational definition of q from a numerical simulation is the distance between successive maxima. This is not *precisely* the quantity we shall solve for in seeking solutions in the form of superposed pulses because, in the simulations, the pulses are slightly distorted from their isolated shapes through mutual interaction. But even for a highly distorted pair state, the difference is less than 1%.

Figure 3 illustrates all of the traveling-wave two-particle solutions to (3) that we have been able to find over the range of domain sizes shown. Solutions are shown with solid or dotted lines as they are linearly stable or unstable, respectively. There is a choice of which of the pair is the follower and which the leader, and we include both cases. So there is generally a pair of values of q at each L, which add up to L. These represent the same state and form a single curved locus in the figure. The

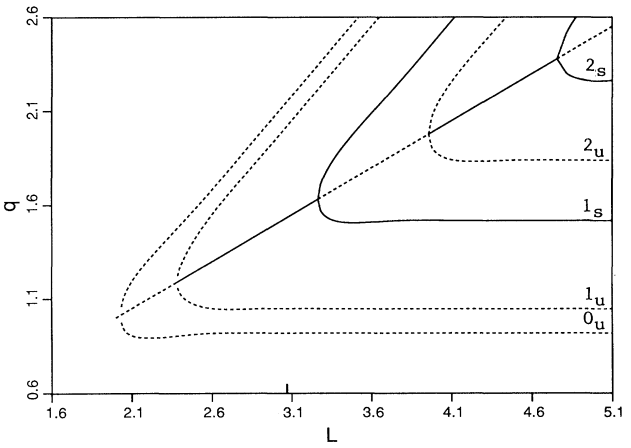

FIG. 3. The family of two-particle solutions found from (3) with parameters $(\nu,\mu,\lambda)=(2,1,1)$. Linear stability is indicated with a solid line, instability with a dashed line. Both q and L are plotted in units of $L_1=\sqrt{2}\pi$. The two-particle solutions disappear at $L=2$ in these units. The first two bifurcating branches should join smoothly at the ends of the first straight dashed-line segment; however, it is difficult numerically to find solutions any closer to the join. The heavy tic mark on the L axis, at $L=3.07$, denotes the edge of the region of stability of the single-particle periodic solution. For larger L, the single-particle solution is always unstable. A family of triplet solutions exists for $L \geq 3$. The first stable triplet solution occurs for $L \approx 3.6$ and has $q_1=q_2=L/3$.

upper portion of such a curved branch is redundant, reflecting a complementary pair separation of $q=L+x_1-x_2$ rather than $q=x_2-x_1$, where the coordinate x_2 is associated with the right-hand particle of the pair and x_1, the left. Similarly, along the main diagonal branch of solutions we have $q=L/2$, where the two values of q are degenerate. This degenerate pair is the formal continuation of a single-particle solution for a domain of size $L/2$ into a periodic pair solution. This solution terminates at $L=2\pi\sqrt{2}$ (normalized to $L=2$ in the figure), where its amplitude tends smoothly to zero. A preliminary description of these two-particle bound states appears in Kawahara and Toh [8], where it is observed that the spectrum of solutions is quantized by virtue of the fact that particles prefer to "sit" in the minima of each other's potential wells.

The single-particle state exists for all L down to $\sqrt{2}\pi$. At a value of about 13.66, it becomes linearly unstable and is thus not realized for greater L. Similarly, we cannot show the triplet family of solutions without complicating our discussion unnecessarily. Much of the structure of the triplet family, which commences at $L=3\sqrt{2}\pi$, may be inferred from a knowledge of the one- and two-particle solutions. For dynamical purposes, one must eventually incorporate all such states into the theory.

To refer to the two-particle solutions, we introduce a taxonomy as follows: Branches bifurcating from the diagonal are numbered sequentially, 1,2,3,.... The stability of the branch is indicated by the subscript u or s, so branches are referred to as 0_u, 1_u, 1_s, 2_u, and 2_s in order of increasing q at the point of bifurcation. Segments of the main diagonal solutions are designated by a superscript as in ${}^1 0_u$, ${}^1 0_s$, ${}^2 0_u$, ${}^2 0_s$, and ${}^3 0_u$ moving upward from the lower left-hand corner. With reference to *this* choice of parameters, the letters s and u denote stability and instability of the respective branches. As we move through parameter space, the topology of the diagram is preserved, but the stability of the various branches is not.

Our main aim here is to develop a quantitative theory of Fig. 3. In this, we have been successful. However, we can also go further and show some numerical results from (2) where we have not yet obtained a full *dynamical* understanding. Consider an evolution experiment from branch 1_u at $L=12$. For an initial condition we have a perturbed localized solution with a maximum relative amplitude perturbation of $\pm 10^{-3}$ induced by adding a bit of the eigensolution of fastest growth rate 1.01. Depending upon the sign of the perturbation, the q of the base state is either decreased or increased. If q is increased, the system rapidly evolves to solution ${}^1 0_s$, approaching it in oscillatory fashion (eigenvalue $-0.429\pm 1.063i$). On the other hand, if q is decreased, the solution evolves to a single-particle state. Since the integral of u is conserved, this may not at first glance appear possible, but what we observe is that the solution generates its own boost, moving to a different reference frame. The value of u far from any particles is thus displaced by an appropriate constant offset to preserve the constancy of the integral. In terms of outcome, a more elementary experiment follows evolution from branch 2_u at $L=18$. In this instance, for decreased q, the trajectory tends to state 1_s in oscillatory fashion ($-0.3358\pm 2.618i$), while evolution with increased q tends to ${}^2 0_s$ monotonically (-0.018).

Many more two-particle experiments could be described, but these two suffice to indicate the range of behavior to be explained. We have done several other experiments with solutions containing as many as five particles. In every instance we have observed, for the parameters $\nu=2$, $\mu=1$, and $\lambda=1$, regardless of initial conditions, the system rapidly locks into a steady-state traveling-wave solution. Such a state is characterized by the existence of an inertial frame in which the solution is steady for large times.

Experiments we have performed for the choice $\nu=1$, $\mu=0.1$, and $\lambda=1$ furnish some interesting points of comparison. The family of two-particle states is little altered from Fig. 3 in structure. However, for a domain somewhat larger than L_2, we find that *all* of the steady-state solutions are linearly unstable for this choice of parameters, foreshadowing the occurrence of chaotic solutions found in the Kuramoto-Sivashinsky equation ($\mu=0$).

With the latter parameter values, evolution of the solution from the state corresponding to 1_s in Fig. 3 (although the s is no longer appropriate) leads to an interestingly disordered state in time and space. We show in Fig. 4 an (x,t) portion from a longer run. There is still a statistically steady state, apart from some *zitterbewegung*, in the sense that the average phase velocity differs by -0.06 from that of the initial state 1_s. The smallness of this difference provides at least one indication that the evolved disorder produces a state which does not stray too far from the (unstable) steady-state profile. It seems reasonable to label this more complex evolution also as a two-particle state (as opposed to one or three). Nonetheless, if we search for a dynamics predicated on relative coordinates p and q, a reduced two-dimensional phase space cannot capture the evident disorder, as noted by Kawahara and Takaoka [19], who attempted to describe the disordered solutions of (2) for the

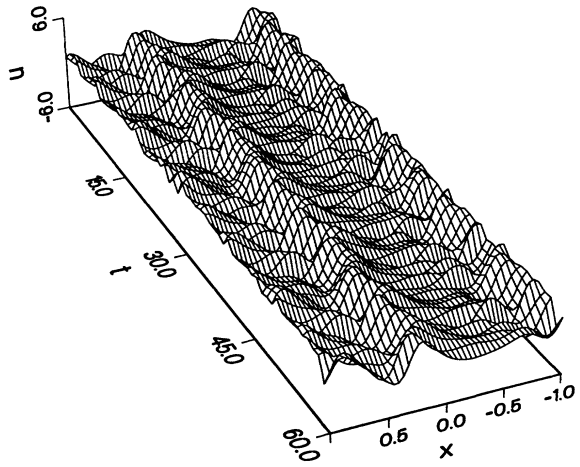

FIG. 4. Disordered solution for (2) with parameters $(\nu,\mu,\lambda)=(1,0.1,1)$.

same parameter choice of $(\nu,\mu,\lambda)=(1,0.1,1)$ with a three-particle ODE model and produced chaotic solutions. Clearly there is more here to be understood than is contained within any discrete description that has been tried so far.

IV. THEORY OF BOUND STATES

Our simulations have all shown that asymptotic states are approached where several pulses are locked into constant relative positions in frames of constant velocity. In this section we give an approximate theory of these bound states. One way to proceed would be to go to a moving frame and look for solutions of the resulting ODE. However, we shall work straight from the PDE in a procedure that will admit immediate generalization to the derivation of equations of motion for localized structures, to which we turn in the next section.

The asymptotic numerical solutions closely resemble superpositions of N of the single pulses $H(\xi)$, with $\xi=x-ct$. We proceed by describing the multipulse solutions as combinations of interacting single pulses $H(\xi-\xi_i)$ centered at the positions ξ_i. When the pulses are far enough apart to make their overlaps weak, we may then express such interacting solutions in the form $\sum_{j=1}^{N}H(\xi-\xi_j)+\mathcal{R}(\xi)$ where $\mathcal{R}$ is a remainder resulting from the fact that, even in this dilute regime, a linear superposition can only be approximate. This form makes no explicit allowance for the main effect of the interactions among pulses, and leaves room for improvement.

The effect of distant pulses locally on a pulse is to alter the local velocity simply by adding a bit to u. Hence, as we find numerically, the velocity of a bound state differs from that of a single pulse, at least when we select the frame in which $\mathcal{R}$ tends to zero as $|\xi|\to\infty$. Therefore, we are well advised in seeking multipulse solutions to change the c in $\xi=x-ct$ to the new speed $c+\Delta c$ say, of the frame in which the lattice of pulses is steady. Of course, we do not know Δc in advance, so we express the change in an open-ended way by seeking a solution of the form

$$u(x,t)=\sum_{j=1}^{N}H(\xi-\xi_j-Y)+\mathcal{R}(\xi-Y)\ , \tag{10}$$

where $\dot{Y}=\Delta c$ is the correction caused by the interactions.

We expect that both $\mathcal{R}$ and Δc are small when the interactions are weak. A measure of smallness is expressed in terms of the typical separation between nearest neighbors, d. If the pulse width is σ, then the smallness is characterized by $\epsilon=\exp(-d/\sigma)$. Both $\mathcal{R}$ and Δc are of this order, as can be confirmed by inspection of the equations. This ordering guides us in rewriting (2) with the help of (3) as

$$\mathcal{L}\mathcal{R}=\tfrac{1}{2}\partial_z\left[\sum_{j\ (\neq k)}\sum_{k=1}^{N}H(z-\xi_j)H(z-\xi_k)-\mathcal{R}^2\right]+\left[\sum_{j=1}^{N}H'(\xi-\xi_j-Y)+\mathcal{R}'\right]\dot{Y}\ , \tag{11}$$

where

$$z=\xi-Y \tag{12}$$

and

$$\mathcal{L}=\lambda\partial_z^4+\mu\partial_z^3+\nu\partial_z^2-c\partial_z+\sum_{j=1}^{N}H(z-\xi_j)\partial_z+\sum_{j=1}^{N}H'(z-\xi_j)\ . \tag{13}$$

The formal procedure suggested by this restatement is the development of $\mathcal{R}$ in ϵ with the requirement that the perturbation equation be solvable in each order. One cannot, however, exclude the possibility that an alternative expansion procedure, such as that from the theory of normal forms, is required for a correct dynamical descripton of systems with Galilean invariance. Even among the authors there is still a divergence of views on this point, but we proceed here with the simpler assumption of a regular ordering since the formal structure which emerges exhibits all the qualitative features of interest and, in the prediction of bound-state particle spacings, gives results only negligibly affected by inclusion of suggested correction terms involving $\dot{Y}$.

To perform the calculations it is helpful to know the adjoint linear operator and its null vectors. This operator is defined by

$$\int\mathcal{Q}\mathcal{L}\mathcal{R}\,dz=\int\mathcal{R}\mathcal{L}^{\dagger}\mathcal{Q}\,dz\ , \tag{14}$$

where the boundary conditions associated with $\mathcal{L}^{\dagger}$ are chosen so that there are no boundary terms in (14).

Let $\mathcal{R}_{\pm}\equiv\lim_{\pm\infty}\mathcal{R}$. Then (5) implies that $\mathcal{R}_{+}=\pm\mathcal{R}_{-}$ and we find that $\mathcal{Q}_{+}=\pm\mathcal{Q}_{-}$ is the boundary condition associated with $\mathcal{L}^{\dagger}$. With these conditions, we see that

$$\mathcal{L}^{\dagger}=\lambda\partial_z^4-\mu\partial_z^3+\nu\partial_z^2+c\partial_z-\sum_{j=1}^{N}H(z-\xi_j)\partial_z\ . \tag{15}$$

Thus, since $\mathcal{L}^{\dagger}1=0$, 1 is evidently a null vector of the adjoint linear operator. We conclude that the integral of the left-hand side of (11) must vanish. Hence so must the integral of the right-hand side. Indeed it does, but this does not add new information and we must inquire whether there are other null vectors such that

$$\mathcal{L}^{\dagger}\tilde{N}=0\ . \tag{16}$$

Generally, this equation can be solved numerically, if we know in advance where the pulses are. For example, numerical solutions of (16) subject to periodic boundary conditions for a sequence of two-particle bound states (known from the numerical solutions) exhibit precisely one null vector, $\tilde{N}$, apart from the constant solution. What is needed, however, is a way to find this null vector without having to specify in advance the solution sought. Fortunately, as for the solutions themselves, solutions for the null vectors $\tilde{N}$ resemble quite closely superpositions of sharply localized features, each identifiable with the single-particle state. This is not surprising, for the form of $\mathcal{L}^{\dagger}$ is reminiscent of the Hamiltonian for a particle moving in a lattice; it consists of a linear differential operator plus a multipeaked potential, $\sum_{j=1}^{N}H(z-\xi_j)$. As in solid-state physics, we can suppose that the eigenfunctions are well approximated in the neighborhood of one peak by the eigenfunction for a "potential" with just

one peak. This corresponds to the tight-binding approximation of solid-state physics.

Let $\mathcal{L}_i^\dagger$ denote the single-particle operator,

$$\mathcal{L}_i^\dagger=\lambda\partial_z^4-\mu\partial_z^3+\nu\partial_z^2+c\partial_z+H(z-\xi_i)\partial_z \ . \tag{17}$$

Then (16) can be written as

$$\mathcal{L}_i^\dagger\tilde{N}=\sum_{j\,(\neq i)} H(z-\xi_j)\partial_z\tilde{N} \ . \tag{18}$$

The right-hand side of this equation is $O(\epsilon)$. Hence we may expect that, in the neighborhood of the pulse centered on ξ_i, $\tilde{N}$ near ξ_i is well approximated by the single-particle equation:

$$\mathcal{L}_i^\dagger\tilde{N}_i=0 \ . \tag{19}$$

We have studied (19) numerically and have found that, apart from the constant solution, which satisfies $\tilde{N}_{i+}=\tilde{N}_{i-}$, there is only one other solution and it satisfies the complementary condition $\tilde{N}_{i+}=-\tilde{N}_{i-}$. This other single-particle null vector is plotted in Fig. 5. For ξ within a few pulse widths σ of ξ_i, this local result is in excellent agreement with the exact null vector. The use of this local solution in the construction of global null vectors is straightforward. To recover the two-particle *periodic* solution of (16) mentioned above from $\tilde{N}_i$, we take the *alternating* sum

$$\tilde{N}=\tilde{N}_i(z-\xi_1)-\tilde{N}_i(z-\xi_2)+O(\epsilon) \ . \tag{20}$$

This produces good agreement with the numerical results. In the case of interacting particles in an unbounded domain, solutions of (16) can be composed as superpositions of the single-particle solution, $\tilde{N}_i$, with either sign and thus, in addition to (20), a symmetric combination would seem admissible. When the size of the domain for the periodic solution is large relative to the scale of the particles, we might expect to recover this indifference to sign, which would have the important consequence of permitting us to predict not only the particle spacing [as we see later in (26)] from the antisymmetric combination, but also the correction to the single-particle reference frame, $\dot{Y}$, from the solvability condition applied to the symmetric form.

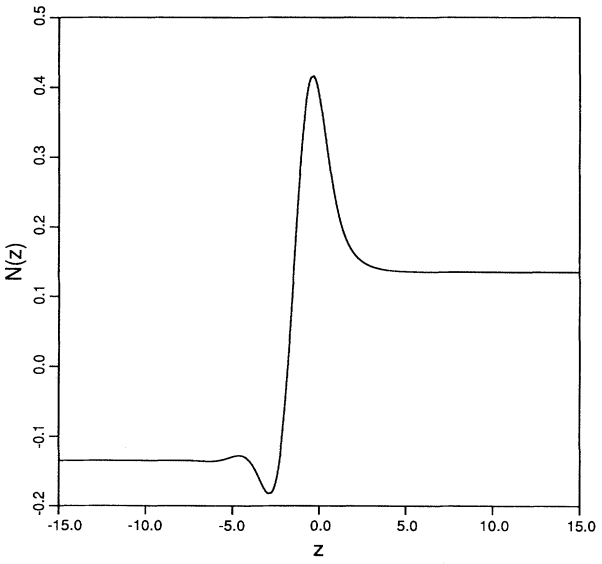

FIG. 5. The normalized adjoint null vector associated with the single-particle operator $\mathcal{L}_i^\dagger$. Parameters are $(\nu,\mu,\lambda)=(2,1,1)$, but the qualitative appearance of the result is preserved for a wide range of parameters.

The structure of the problem is clarified upon noting that we have the evident identity $\mathcal{L}_i 1=H'(z-\xi_i)$, and that we readily verify that $\mathcal{L}_i H'(z-\xi_i)=0$, where $\mathcal{L}_i$ is defined in analogy to $\mathcal{L}_i^\dagger$ [see (29a)]. These relations are summarized in

$$\mathcal{L}_i\begin{bmatrix}H'\\1\end{bmatrix}=\begin{bmatrix}0&0\\1&0\end{bmatrix}\begin{bmatrix}H'\\1\end{bmatrix} , \tag{21}$$

which is characteristic of systems with Galilean invariance. There is here only one null vector. By contrast, the adjoint single-particle operator has two null vectors, 1 and $\tilde{N}_i$. The integral of u introduced in (4) is called a distinguished functional in the sense that, for systems possessing a Hamiltonian structure, its conservation is not related to any Noether symmetry. In our problem there seems to be a relation between this functional and the adjoint null vector 1 which arises from the Galilean invariance. Though our problem is not Hamiltonian, this functional and $\dot{Y}$ are reminiscent of action-angle variables.

Now, we return to (11). The idea of the perturbation theory underlying the present procedure is that $\mathcal{R}$ is small and so, in first approximation, we neglect the last two terms on the right. Moreover, the exponential decay of the pulse shape means that we can restrict our attention in this approximation to values of $j=i\pm1$ so that the solvability condition in leading order becomes

$$\sum_i\int\tilde{N}\{H(z-\xi_i)[H(z-\xi_{i-1})+H(z-\xi_{i+1})]\}'dz=0 \ . \tag{22}$$

Note that the terms involving $\tilde{N}H'(z-\xi_i)$ cancel identically.

Only terms with $|i-j|=1$ enter to this order so that the nearest-neighbor approximation is a consequence of the development. The higher-order interactions, being smaller by at least a factor ϵ, are introduced in calculating the higher-order approximations for $\mathcal{R}$ via the solvability condition. We shall not carry the calculation that far here, but we should stress that the need to go to the next order to complete the analysis of a formal expansion in ϵ is a complication not easily surmounted in a general way.

We define

$$F(\Delta_{ij})\equiv\int_{-\infty}^{\infty}[H(z-\xi_i)H(z-\xi_j)]'\tilde{N}_1(z-\xi_i)dz \ , \tag{23}$$

where

$$\Delta_{ij}=\xi_i-\xi_j \ . \tag{24}$$

A numerical computation of F is seen in Fig. 6 for our canonical choices of parameters $(\nu,\mu,\lambda)=(2,1,1)$, but the same qualitative structure is obtained over a wide range. Since the pulse is exponentially small far from its core, the function H is easily approximated by linear theory. The roots of the indicial equation resulting from linearization of the associated ODE determine the exponentials in question. We find that F is well approximated by the simple asymptotic form

$$F(Z)=f_L e^{-\beta_L Z}\cos(\omega_L Z+\phi_L) \ , \tag{25a}$$

$$F(-Z)=f_R e^{-\beta_R Z}\cos(\omega_R Z+\phi_R) \ , \tag{25b}$$

for $Z\to+\infty$. (The subscripts L and R stand for left and right outer limits of the single-pulse solution.) For our example, the constants turn out to be $f_R=-141.78$, $f_L=-304.49$, $\beta_R=1.1869$, $\beta_L=1.0934$, $\omega_R=0$, $\omega_L=1.8439$, $\phi_R=0$, and $\phi_L=-1.1531$.

Application of (20) and (23) reduces (22) after some manipulation to the condition

$$F(q)-F(-q)+F(q-L)-F(L-q)=0 \ , \tag{26}$$

where the two particles are assumed to have separation q in a domain of size L. The alternating signs in (26) arise from the antisymmetric combination used in composing $\tilde{N}$.

Note that $q=L/2$ satisfies (26) identically; thus we always obtain a pair solution with spacing of half the domain size although, as we have already seen, the PDE has a sequence of critical domain sizes, L_n, at which N-particle solutions are first admitted. The family of two-particle periodic solutions predicted by (26) with parameters $(\nu,\mu,\lambda)=(2,1,1)$ is shown in Fig. 7, where both q and L are plotted in units of $L_1=\sqrt{2}\pi$. The comparison of this with the actual bound states shown in Fig. 3 gives remarkable agreement for $q(L)$, except for the first bifurcating branch, for which the pulse separation is not very great. We return to a discussion of the predicted stability of these states in the next section on the dynamics of pulses.

Figure 8 displays two-particle periodic solutions predicted by (26) with parameters $(\nu,\mu,\lambda)=(1,0.1,1)$. Again, q and L are plotted in units of L_1 $(=2\pi)$. Note

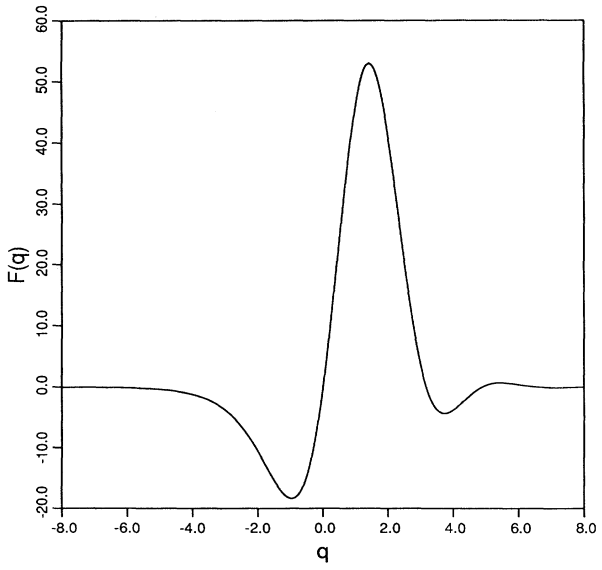

FIG. 6. The function $F(q)$ from (19) for parameters $(\nu,\mu,\lambda)=(2,1,1)$.

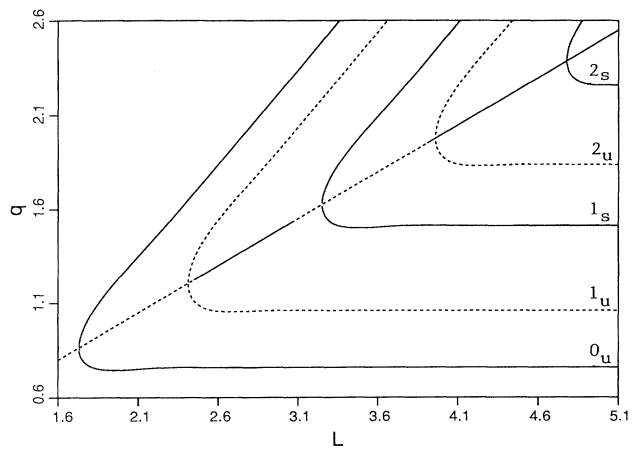

FIG. 7. The family of two-particle periodic solutions predicted by (26) with parameters $(\nu,\mu,\lambda)=(2,1,1)$. Linear stability is indicated with a solid line, instability with a dashed line. Both q and L are plotted in units of $L_1=\sqrt{2}\pi$.

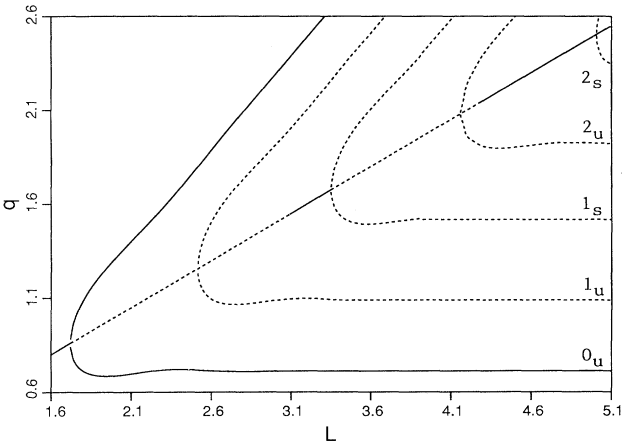

FIG. 8. The family of two-particle periodic solutions predicted by (26) with parameters $(\nu,\mu,\lambda)=(1,0.1,1)$. Linear stability is indicated with a solid line, instability with a dashed line. Both q and L are plotted in units of $L_1=2\pi$. Note that the fixed-point structure is only slightly changed when compared to Fig. 7. For the PDE, the stability picture is more complicated, but these predictions for $q(L)$ are in excellent agreement, except, again, for the first branch.

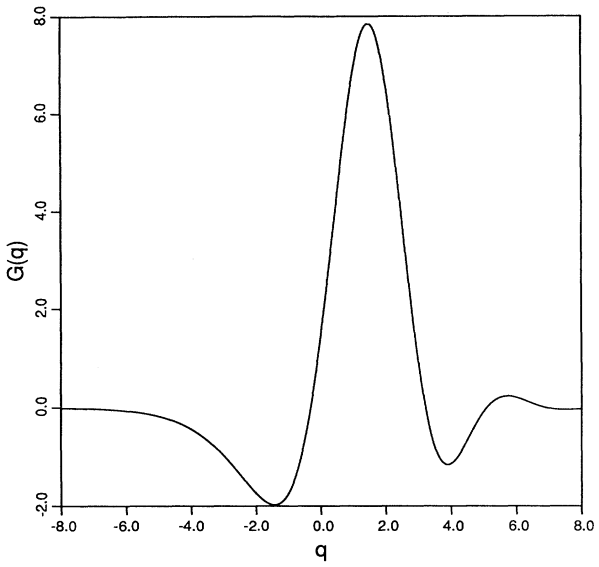

FIG. 9. The function $G(q)$ from (34) for parameters $(\nu,\mu,\lambda)=(2,1,1)$.

that the locations of the branches are only slightly changed compared to Fig. 7. The predictions for $q(L)$ give excellent agreement, except, again, for the first branch. (In contrast with the results found here, for the PDE, there are ranges of domain size in which *all* of the branches appear to be unstable.)

We were also surprised to observe that, with regard to the $q(L)$ diagram for the family of two-particle states, there is nothing singular about passing to $\mu=0$. The entire apparatus described in this section carries through with a result not very different from Fig. 8. In short, the impression from the numerical simulations—that the solutions turn into lattices of single pulses when expressed in formulas, as here— is well verified over a wide range of parameters both qualitatively and quantitatively.

V. PULSE DYNAMICS

A. Equations of motion

Apart from some possible transient behavior, our numerical simulations look as if there were simply a number of pulses, or particles, moving under their mutual interactions until they finally form a stable lattice. These collective asymptotic states are steady, but in a different frame from that preferred by a single pulse. In the preceding section, we showed how these lattices can be understood as bound states of single pulses. Now, we try to generalize that effective-particle approach to the derivation of equations of motion of the individual pulses as they move under their mutual interactions to form the bound states. As before, each particle shall be the pulse found as the homoclinic solution of Eq. (2), shown in Fig. 2 for $\lambda=\mu=1$ and $\nu=2$ and found to have $c=5.4545$.

We need to allow for two new features of the problem in generalizing (10). Prior to achieving the steady bound state, the system is not moving globally at constant speed, so we shall not fix the time dependence of Y in (10) in an *a priori* way, as we did in the preceding section. More importantly, the pulses are moving and accelerating at different rates prior to forming a bound state, and we must allow for this richer behavior. We could proceed from the point of view of fields by letting Y depend weakly on position, and finding a PDE for this new field. But we prefer the particle viewpoint in which we concentrate on the vicinity of one pulse at a time. So we make a Galilean transformation of (10) to the local frame around the ith pulse. In fixing our attention on the neighborhood of the ith pulse, we continue to suppose that the pulses are widely separated with a typical interpulse distance much greater than the pulse width (small ϵ).

When we boost the ansatz (10) to a frame suitable for a particular pulse with the transformation $u(z,t)\to u(z-x_i)+V_i$, it becomes

$$u(x,t)=\sum_{j=1}^{N} H(\xi-X_j-Y)+V_i+\mathcal{R}(\xi-Y-X_i,t)\ , \quad (27)$$

where X_j are the positions of the pulses in the new frame.

As before, we shall try to make the error term $\mathcal{R}$ small where the measure of this smallness is $\epsilon=\exp(-d/\sigma)$, with d as a typical separation between pulses whose width is σ. We suppose that $\mathcal{R}$ covers errors of this size such as the neglect of pulse distortions that arise in the interactions.

If we were to proceed as in regular perturbation theory, we would find that $\mathcal{R}$ is not small. Our aim, as usual in singular perturbation theory, is to let the group parameters depend on time so as to make the perturbation theory work. In the spirit of singular perturbation theory we determine these time dependences through solvability conditions that render the asymptotic calculation of $\mathcal{R}$ possible. These solvability conditions are equations of motion for the pulses. The parameters we introduce into (27) which break the Galilean and translational invariances of the problem are, in other language, simply the unfolding parameters of a singularity of codimension 2.

We insert (27) into (2) and discover that $\mathcal{R}$ and $\dot{Y}$ are of $O(\epsilon)$. So to leading order, for the neighborhood of the ith pulse, we have

$$\begin{aligned}\mathcal{L}_i\mathcal{R}=&-\dot{V}_i-(V_i-V_{i+1})H'(\xi-Y-X_{i+1})\\&-(V_i-V_{i-1})H'(\xi-Y-X_{i-1})-\dot{Y}H'(\xi-Y-X_i)\\&-\tfrac{1}{2}\sum_{j\ (\neq k)}\sum_{k}[H(\xi-Y-X_j)H(\xi-Y-X_k)]'\ ,\end{aligned} \quad (28)$$

where

$$\begin{aligned}\mathcal{L}_i=&-c\partial_z+\nu\partial_{zz}+\mu\partial_{zzz}+\lambda\partial_{zzzz}\\&+H'(z-X_i)+H(z-X_i)\partial_z\ ,\end{aligned} \quad (29a)$$

$$z=\xi-Y \tag{29b}$$

and we have used, as a property of the local boost,

$$\dot{X}_i=V_i \ . \tag{30}$$

As in the preceding section, only the nearest-neighbor interactions enter in this order. In (28) we have not included additional terms of the form $\dot{Y}H'(\xi-Y-X_{i\pm1})$ which are formally of the same order as those involving the velocity differences, $V_i-V_{i\pm1}$. For simplicity we keep the only leading order $\dot{Y}$ term, but, in principle, if we keep the terms involving velocity differences, there is no reason to exclude the other $\dot{Y}$ terms.

The operator $\mathcal{L}$ and its adjoint, $\mathcal{L}^\dagger$, have already been discussed. In particular, 1 is a null vector of the adjoint linear operator and must be orthogonal to the right-hand side of (28). Since we have allowed ourselves the liberty of examining this only in the neighborhood of the ith pulse, we have to apply this condition with judgement. The integral implied in the inner product is over the whole domain, and so the contributions from each pulse neighborhood must be included. Our first solvability condition is then

$$\sum_{i=1}^{N}\dot{V}_i=0 \ . \tag{31}$$

The second solvability condition gives the equations of motion of the pulses. The procedure is exactly the same as we used in deriving the equilibrium condition above, except that now it yields

$$\dot{V}_i=\mathcal{F}(\Delta X_i,\Delta X_{i+1},\Delta V_i,\Delta V_{i+1},\dot{Y}) \ , \tag{32}$$

where $\Delta X_i=X_i-X_{i-1}$ and $\Delta V_i=V_i-V_{i-1}$. The interparticle force is

$$\begin{aligned}\mathcal{F}=&F(\Delta X_i)+F(-\Delta X_{i+1})+\Delta V_i G(\Delta X_i)\\&-\Delta V_{i+1}G(-\Delta X_{i+1})+\dot{Y}G(0)\end{aligned} \tag{33}$$

with F as in the steady case and

$$G(q)=-\int_{-\infty}^{\infty}\tilde{N}(z)H'(z+q)dz \ . \tag{34}$$

The function G has a more complicated asymptotic behavior than F, although a form such as (25) can be fitted for a moderate range in z. Accurate computation of G for large argument (e.g., greater than 15 with the present parameters) is a delicate matter. Results from numerical integration of (34) are displayed in Fig. 9. With these explicit results, we have completed a specification for the dynamical equations of N pulses.

B. Two-body problem

The case of two pulses illustrates nicely the formation of bound states. For $N=2$, we introduce the new coordinates and velocities

$$\begin{aligned}&Q=\tfrac{1}{2}(X_1+X_2) \ , \quad q=X_2-X_1 \ ,\\&P=\tfrac{1}{2}(V_1+V_2) \ , \quad p=V_2-V_1 \ .\end{aligned} \tag{35}$$

Then the relative motion is governed by

$$\dot{q}=p \ , \tag{36a}$$

$$\dot{p}=F(q)-F(-q)+p[G(q)+G(-q)] \ , \tag{36b}$$

while the motion of the center of mass and of the global variable Y is given by

$$\dot{Q}=P \ , \tag{37a}$$

$$\dot{P}=0 \ , \tag{37b}$$

$$2G(0)\dot{Y}=[F(q)+F(-q)]+p[G(q)-G(-q)] \ . \tag{37c}$$

The system coordinate Y remains in the problem, unlike what we are used to in ordinary dynamical problems. The reason is that the "particles" of our system do not possess fore-aft symmetry. Hence, there is no immediate analog of Newton's Third Law here. The two particles thus chase each other until frictional effects on the system bring them to a terminal velocity characteristic of their final state. The term $\dot{Y}$ is the velocity correction from the one-particle state to this new bound state, and it plays the key role in the adjustment of frames.

Equations (36) may be solved independently of (37). In Fig. 10, we show the positive q portion of the phase portrait for Eqs. (36). We see a few of the countably infinite fixed points that arise in (36). These are alternately stable foci (or spiral points) and saddle points. The "ground" state of the implied bound pair has a separation of about 3.3482. (Note that a bound state of (36) corresponds to a double-pulsed homoclinic solution of the associated ODE, which is also the associated ODE for other PDE's, including some without Galilean invariance [15,23].) This solution can be identified with the previous periodic solution branch from the PDE labeled 0_u in the limit of large L. The separation there approaches a limiting value of 4.065. The disparity in these values is attributable to

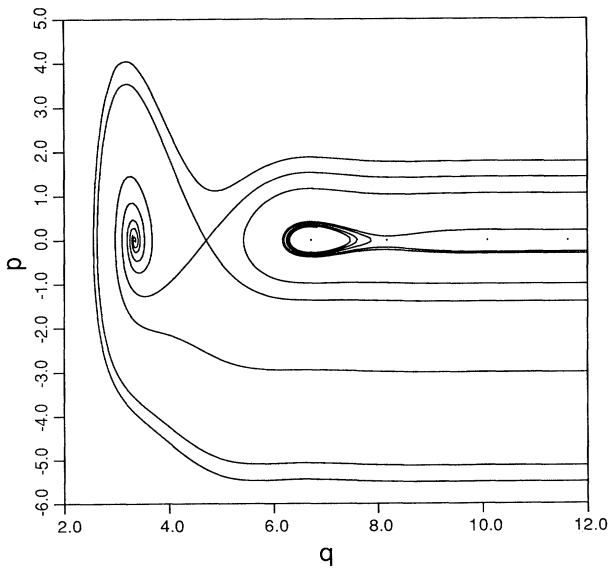

FIG. 10. A portion of the phase portrait for Eqs. (36) showing the fixed points and a few sample orbits.

the effects of distortion when the particles are so close compared to their natural width, σ. This marked overlap presumably also accounts for the opposite conclusions regarding the stability.

When, in a two-body interaction, a bound state is formed, the pair is able to go to the correct frame because of the $\dot{Y}$ term in (32). Once it is there, (37c) is satisfied identically, with constant $\dot{Y}$. The frame velocity for a bound pair is $c+\dot{Y}$. From (37c), we get $\dot{Y}=[F(q)+F(-q)]/[2G(0)]$. This result is consistent with the velocity correction being $O(\epsilon)$, as we have assumed. This is in agreement with the numerical experiments.

We cannot resist also showing what the theory predicts about hard collisions, when the pulses approach to within a distance σ from each other. Of course, the approximations used do not apply in that case. Moreover, since the pulses now may overlap, our original ansatz has to be adjusted by subtracting the overlap term. When we do this, we get the phase portrait shown in Fig. 11, on a scale larger than in Fig. 10. An additional saddle point appears at $(q=0, p=0)$, and the topology of the solution curves implies the existence of a critical relative velocity p_c (about 11.75 for the parameters of this example). Below p_c (in magnitude), particles approaching each other from large initial separation are reflected, while above it they penetrate to the other side.

A more telling comparison of results of the effective-particle theory with numerical experiments based on (2) other than just the nature of the bound states is desirable. We need to know whether the evolution to the bound states by the capture process just described is realizable. For a two-pulse state with large separation, the instability

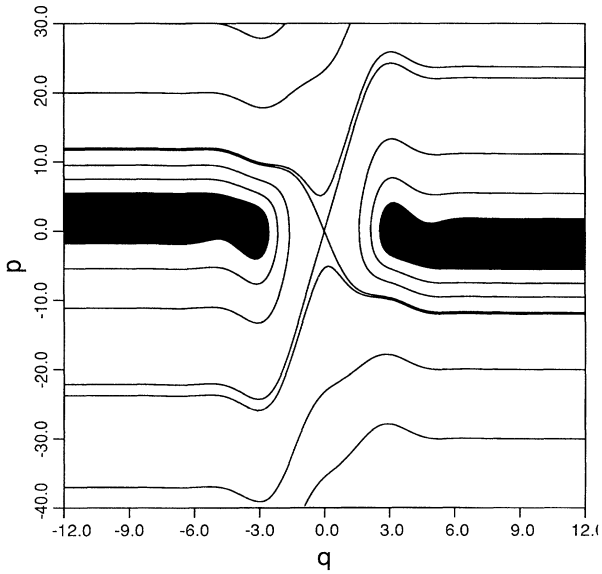

FIG. 11. The phase portrait for the two-body problem suggested by Eqs. (36) for larger values of incident velocity. The shaded regions are illustrated in the more detailed view of Fig. 10.

to the formation of other pulses might be rapid enough to make the two-body discussion of the scattering process unrealistic. As we have already mentioned, such comparisons are made delicate by the question of boundary conditions. The simulations of (2) with the longest time of validity are those with periodic boundary conditions. To facilitate comparisons, we recast the scattering theory in terms of periodic boundary conditions.

To study the two-body problem with periodic boundary conditions, we return to the many-body equations (17)–(21) and simply add the constraints

$$\Delta X_i+\Delta X_{i+1}=L, \quad \Delta V_i+\Delta V_{i+1}=0 . \tag{38}$$

Then, upon indexing the two particles with $i=1$ and $i=2$, we find the equations

$$\dot{X}_i=V_i , \tag{39a}$$

$$\dot{V}_i=F(-\epsilon_i q)+F(\epsilon_i(L-q))-\epsilon_i pG(-\epsilon_i q) -\epsilon_i pG(\epsilon_i(L-q))+\dot{Y}G(0) , \tag{39b}$$

where ϵ_i is $+1$ for $i=1$ and -1 for $i=2$, and $\dot{V}_1+\dot{V}_2=0$.

Referring back to Fig. 7, we see that there is qualitative agreement in the sequence of alternating stable and unstable branches, except for the first. In detail, however, the comparison presents difficulties. The ODE branch 1_u, for example, is a saddle point with a pair of real eigenvalues of opposite sign ($[1.46, -2.18]$ at $L=12$). In decreasing order of the real part of the eigenvalues of the PDE, by contrast, for the same value of L, we find eigenvalues of 1.01 and $-1.37\pm0.149i$. The latter set cannot, of course, be captured by a two-dimensional relative coordinate phase space. A second example is the 2_s branch of the ODE which is a stable spiral, whereas the PDE exhibits a pair of negative, but real eigenvalues. (Note that the PDE always has a zero-eigenvalue translational mode and in the ODE set, this is simply the Y degree of freedom.)

C. *N*-body complexity

A discussion of the dynamics with only a few, but more than two, bodies is hopelessly complex, as in all dynamics problems. But for large N, we are immediately conducted to interesting results on setting $V_i=V_0=\text{const}$ and $-\dot{Y}G(0)\equiv A=\text{const}$. This corresponds to a constant velocity of the whole pattern of N pulses in an asymptotic steady state. Then Eqs. (30) and (32) reduce to the pattern map:

$$F(-\Delta_{n+1})=A-F(\Delta_n) , \quad \Delta_n\equiv\Delta X_n\equiv X_n-X_{n-1} . \tag{40}$$

For an infinite train of pulses, there is always a fixed point of the map corresponding to uniformly spaced

pulses, and (40) is a relation between the spacing and A.

The map (40) has the same form as the Poincaré map for flows arising from ODE's of the general form (3), when the parameaters λ, μ, and ν are close to the ones used by us. Such maps can be derived using the arguments of Shil'nikov [20] or of Melnikov [24]. In the present work, this map tells us how successive pulses are spaced. It is known that such spacings may be uniform, periodic, or *spatially* chaotic (when $\beta_L/\beta_R < 1$, as in our case).

For the map given by (40), we may solve $\Delta_{n+1}=\Theta(\Delta_n)$. Instability of the fixed point $\Delta_n \equiv \Delta_* = \text{const}$ depends on the parameter $\alpha=\Theta'(\Delta_*)$. The necessary and sufficient condition for instability of the map is $|\alpha|>1$ [25]. For pulse trains without Galilean invariance, the condition for instability is $1+\alpha<0$ [15]. For the present case, with Galilean invariance, we again have the condition $1+\alpha<0$ for instability with, in addition, the condition that $G(\Delta_*)+G(-\Delta_*)>0$. The latter may be interpreted as a condition of negative effective friction. The instability of the uniformly spaced pattern leads to a pairing of pulses, which doubles the spatial period of the pattern.

VI. CONCLUSIONS

When a fluid flows down an inclined plane, waves grow to large amplitude through an instability. The nonlinear development of such instabilities given by Benney [5] leads to the dynamics of the envelope of a packet of growing waves. For scales much greater than the layer thickness, the essence of the dynamics is contained in the phase of the envelope function. Thus Benney's Eq. (3) foreshadows the modern development of phase dynamics and forms a link between theories of solitons and dissipative structures [2].

We have seen that numerical experiments on this equation reveal the formation of localized persistent structures and evoke the vision that the complicated dynamics emerging from (3), and indeed from the nonlinear development of instabilities of extended systems generally, give rise to a kind of particle dynamics made up of solitary waves. Though the systems we are discussing are not endowed with integrability, these solitary waves, as we have seen, are stable—perhaps sufficiently so to be called solitons in some lexicons. In any case, the description in terms of solitary waves leads naturally to a discretization; that is, to a description of the dynamics in terms of several independent structures. Thus we encounter here, as in many branches of physics, an interesting dichotomy between the particulate and the continuum descriptions.

We shall not attempt to summarize the developments that we have already detailed here. We should simply like to conclude by recalling that the formation and stability properties of the bound states as outlined above should help in understanding the qualitative appearances of regular arrays of pulses and other striking patterns that come up in unstable extended systems in a variety of contexts, particularly in fluid dynamics. Indeed, we could have come full circle and taken the many-body case over to the continuum limit, but we leave that step to the reader's imagination. However, it should be clear that by taking such a limit of our particulate descriptions, (32) and (33), as if they were difference equations, we can make another contact with the theory of phase dynamics [26].

For these various reasons, it has seemed to us worthwhile to have in hand a suitable description of the Galilean dynamics of interacting localized structures. Though there remain some particular points to be explored in these problems, we think we have taken the calculations far enough to reveal that there are some general features of interest in such problems. Beyond that, we may hope that, just as many ODE's have in common Poincaré maps of the same form, so too will classes of PDE's share a common set of dynamical equations for their localized structures. Thus the kind of particle dynamics that we have described here may underlie a possible classification of classical nonlinear field theories.

ACKNOWLEDGMENTS

We are grateful to E. Meron for helpful discussions at the outset of this work. We also thank J. Rinzel for his observations and N. Baker for availing us of his computer code. It is a pleasure to acknowledge support of our collaboration on this project from both the NSF under Grant No. PHY 90-07764 and the U.S. Air Force Office of Scientific Research under Contract No. AFOSR-89-0012. Also, G.I. would like to thank the Office of Naval Research for its support under Contract No. N00014-90-J-1201 with Scripps Institute of Oceanography for the development of numerical methods used in the study reported here.

[1] *Nonlinear Evolution of Spatio-Temporal Structures in Dissipative Continuous Systems,* Vol. 255 of *NATO Advanced Study Institute Series B: Physics,* edited by F. H. Busse and L. Kramer (Phenum, New York, 1990).

[2] P. Manneville, *Dissipative Structures and Weak Turbulence* (Academic, New York, 1990).

[3] Y. Kuramoto, *Chemical Oscillations, Waves and Turbulence* (Springer, Berlin, 1984).

[4] G. B. Whitham, *Linear and Nonlinear Waves* (Wiley-Interscience, New York, 1974).

[5] D. J. Benney, J. Math. Phys. **45**, 150 (1966).

[6] J. Topper and T. Kawahara, J. Phys. Soc. Jpn. **44**, 663 (1978).

[7] S. Toh and T. Kawahara, J. Phys. Soc. Jpn. **54**, 1257 (1985).

[8] T. Kawahara and S. Toh, Phys. Fluids **31**, 2103 (1988).

[9] *Solitons and Coherent Structures,* edited by D. K. Campbell, A. C. Newell, R. J. Schreiffer, and H. Segur [Physica (Amsterdam) **18D** (1986)].

[10] M. J. Ablowitz and H. Segur, *Solitons and the Inverse*

Scattering Transform (Society for Industrial and Applied Mathematics, Philadelphia, 1981).
[11] R. Rajaraman, Phys. Rev. D **15**, 2806 (1977).
[12] C. Elphick and E. Meron, Phys. Rev. A **40**, 3226 (1989).
[13] C. Elphick and E. A. Spiegel, in *General Circulation of the Oceans,* Woods Hole Oceanographic Institution Technical Report WHOI-89-54, edited by G. Flierl (Woods Hole Oceanographic Institution, Woods Hole, MA, 1989).
[14] P. Coullet, C. Elphick, and D. Repaux, Phys. Rev. Lett. **58**, 431 (1987).
[15] C. Elphick, E. Meron, and E. A. Spiegel, Phys. Rev. Lett. **61**, 496 (1988).
[16] D. J. Kaup and A. C. Newell, Proc. R. Soc. London A **361**, 413 (1978).
[17] V. I. Karpman, Zh. Eksp. Teor. Fiz. **77**, 114 (1979) [Sov. Phys.—JETP **50**, 58 (1979)].
[18] G. L. Lamb, *Elements of Soliton Theory* (Wiley-Interscience, New York, 1980).
[19] T. Kawahara and M. Takaoka, Physica D **39**, 43 (1989).
[20] A. Arneodo, P. H. Coullet, E. A. Spiegel, and C. Tresser, Physica (Amsterdam) **14D**, 327 (1985).
[21] M. Rabinovich (private communication).
[22] D. D. Joseph, *Stability of Fluid Motions* (Springer-Verlag, New York, 1976), Vol. 1.
[23] J. Evans, N. Fenichel, J. Feroe, SIAM J. Appl. Math. **42**, 219 (1982); J. Feroe, *ibid.* **42**, 235 (1982).
[24] P. Coullet and C. Elphick, Phys. Lett. A **121**, 233 (1987).
[25] P. Coullet and J.-P. Eckmann, *Iterated Maps on the Interval,* Vol. 1 of *Progress in Physics,* edited by A. Jaffe and D. Ruelle (Birkhäuser, Boston, 1980).
[26] S. Fauve, in *Chaos,* Woods Hole Oceanographic Institution Technical Report WHOI-85-36, edited by G. Veronis (Woods Hole Oceanographic Institution, Woods Hole, MA, 1985).